Journal of Medicinal Chemistry

ARTICLE

pubs.acs.org/jmc

Magnesium Chelating 2-Hydroxyisoquinoline-1,3(2*H*,4*H*)-diones, as Inhibitors of HIV-1 Integrase and/or the HIV-1 Reverse Transcriptase Ribonuclease H Domain: Discovery of a Novel Selective Inhibitor of the Ribonuclease H Function

Muriel Billamboz,[†,‡] Fabrice Bailly,[†,‡] Cédric Lion,[†,‡] Nadia Touati,[†,§] Hervé Vezin,[†,§] Christina Calmels,[∥] Marie-Line Andréola,[∥] Frauke Christ,[⊥] Zeger Debyser,[⊥] and Philippe Cotelle*[,†,‡]

[†]Université Lille Nord de France, F-59000 Lille, France

[‡]USTL, EA 4478 Chimie moléculaire et formulation, F-59650 Villeneuve d'Ascq, France

[§]USTL, UMR CNRS 8516, F-59650 Villeneuve d'Ascq, France

[∥]Institut Fédératif de Recherches "Pathologies Infectieuses et Cancers" (IFR 66), MCMP-UMR 5234 CNRS, Université Victor Segalen Bordeaux 2, F-33076 Bordeaux, France

[⊥]Molecular Medicine, K. U. Leuven and IRC KULAK, Kapucijnenvoer 33, B-3000 Leuven, Flanders, Belgium

Supporting Information

ABSTRACT: 2-Hydroxyisoquinoline-1,3(2*H*,4*H*)-dione was recently discovered as a scaffold for the inhibition of HIV-1 integrase and the ribonuclease H function of HIV-1 reverse transcriptase. First, we investigate its interaction with Mg^{2+} and Mn^{2+} using different spectroscopic techniques and report that 2-hydroxyisoquinoline-1,3(2*H*,4*H*)-dione forms a 1:1 complex with Mg^{2+} but a 1:2 complex with Mn^{2+}. The complex formation requires enolization of the ligand. ESR spectroscopy shows a redox reaction between the ligand and Mn^{2+} producing superoxide anions. Second, 2-hydroxyisoquinoline-1,3(2*H*,4*H*)-dione, its magnesium complex, and its 4-methyl and 2-hydroxy-4-methoxycarbonylisoquinoline-1,3(2*H*,4*H*)-diones were tested as inhibitors of HIV-1 integrase, reverse transcriptase ribonuclease H, and DNA polymerase functions. Their antiviral activities were evaluated and 2-hydroxy-4-methoxycarbonyl-isoquinoline-1,3(2*H*,4*H*)-dione was found to inhibit the viral replication of HIV-1 in MT-4 cells. Cross-resistance was measured for this compound on three different viral strains. Experimental data suggest that the antiviral activity of 2-hydroxy-4-methoxycarbonylisoquinoline-1,3(2*H*,4*H*)-dione is probably due to the RNase H inhibition.

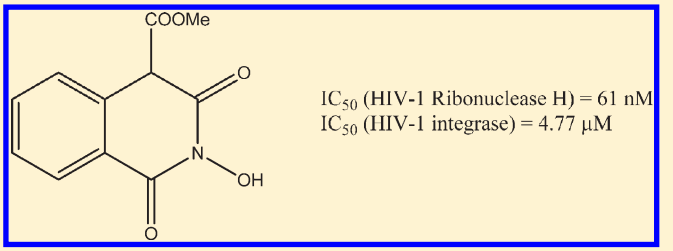

INTRODUCTION

The three HIV-1 enzymes, namely protease, reverse transcriptase, and integrase, have emerged as ideal targets for the development of inhibitors of HIV-1 replication. Anti-HIV drugs targeting these enzymes have been approved for use in the treatment of HIV infection.[1] However, the emergence of drug resistance can attenuate the efficacy of antiretroviral treatment. To suppress these drug-resistant variants, novel anti-HIV drugs that block new targets or several targets simultaneously are urgently needed.

Among these new strategies, the development of inhibitors of integrase (IN) and of the ribonuclease H (RNase H) function of reverse transcriptase (RT) has been proposed.[2] Indeed, HIV-1 integrase and the RNase H domain of HIV-1 RT exhibit striking similarities of structure and function,[3,4] justifying the biological evaluation of newly synthesized compounds on these two viral enzymatic targets.[5,6]

Reverse transcription is performed by reverse transcriptase. RT combines two distinct enzymatic activities, a DNA polymerase activity (N-terminal two-thirds) and a RNase H activity that cleaves the RNA strand of a RNA/DNA hybrid (C-terminal one-third).

IN inserts the viral DNA into the host cellular genome through a multistep process that includes two catalytic reactions: 3′-endonucleolytic processing at both ends of the viral DNA (3′-P) and joining of the 3′-processed viral DNA and host chromosomal DNA (strand transfer: ST).

To date, no X-ray structure of the entire HIV-1 IN with or without substrate is available. Fifteen X-ray structures of the core domain, with and without intact C- or N-terminal domains, have been solved. In these cases, only one Mg^{2+} ion bound by D64 and D116 has been found in the active site of IN.[7−13] However, there is growing evidence in support of a two-metal ion theory. For instance, X-ray structures of ASV integrase with Cd^{2+} or Zn^{2+} show a second binding site between D64 and E157,[14] and

Received: November 16, 2010
Published: March 02, 2011

dx.doi.org/10.1021/jm1014692 | *J. Med. Chem.* 2011, 54, 1812–1824

Scheme 1. HIV-1 RNase H and IN Inhibitors

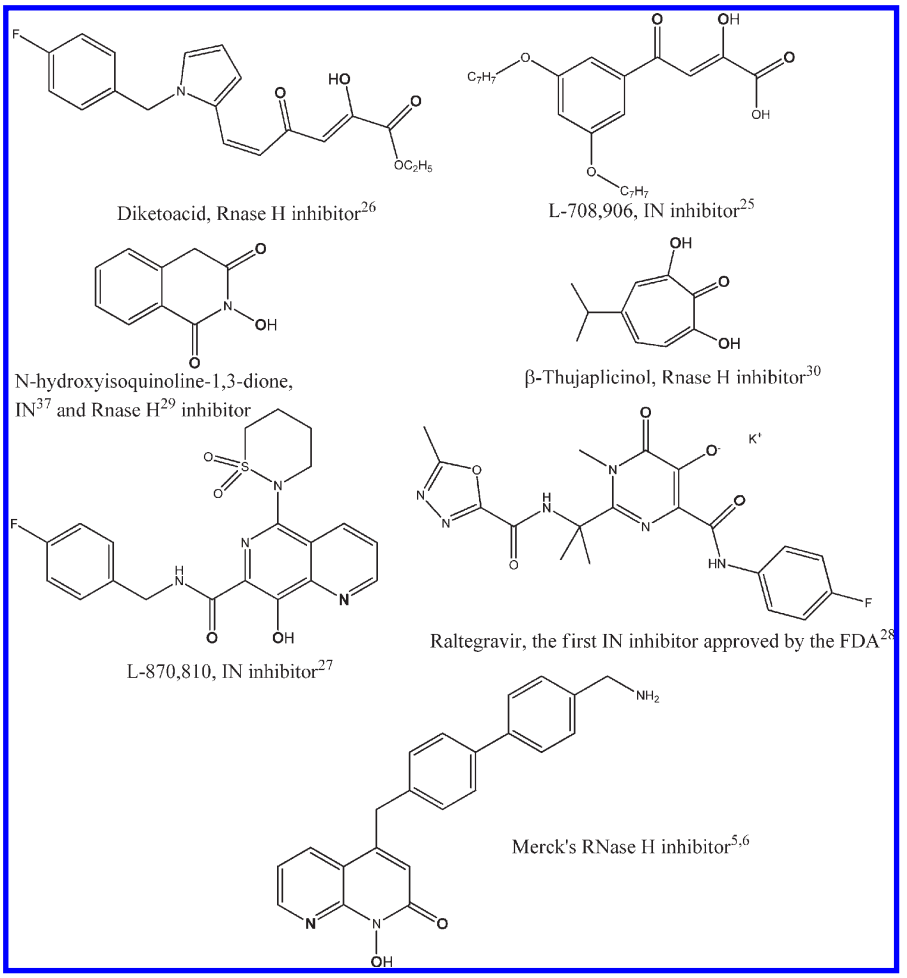

most molecular docking studies consider that IN may welcome two Mg^{2+} ions in its active site. In this hypothesis, the two metal ions should be separated by 3.6 to 3.7 Å. Very recently, Hare et al. reported the crystal structures of full-length prototype foamy virus (PFV) integrase-DNA complexes with various HIV-1 integrase inhibitors, exhibiting two metal ions in the strand transfer active site (Mg^{2+} or Mn^{2+}).[15]

The structure of the HIV-1 RNase H domain has been determined from crystals of the intact enzyme, from the isolated RNase H domain, and from cocrystals of HIV-1 RT and substrate.[16−19] The active site of the RNase H function contains four acidic residues, D443, E478, D498, and D549, that likely coordinate two divalent metal ions that are essential for catalysis, with an intermetallic distance of 4 Å.[16] In a cocrystal structure of full-length HIV-1 RT in a ternary complex, a single Mg^{2+} ion was observed.[20] The similar RNase H domain of *E. coli* binds one or two divalent cations; however, the most recent cocrystal structures of the B. halodurans and human RNase H with bound substrates strongly suggest that RNase H uses a two-metal ion mechanism of catalysis.[21,22] As demonstrated by a NMR study of the RNase H domain, the two Mg^{2+} binding sites present very different dissociation constants, showing that both sites are largely unoccupied under physiological conditions in the absence of substrate.[23]

The design of IN and RNase H inhibitors is therefore strongly related to their ability to bind two Mg^{2+} ions separated by 3.6−4.0 Å.[24] Several inhibitors (Scheme 1) characteristically present three aligned heteroatoms (bold atoms, mainly three oxygens). Typical examples are members of the diketoacid family (DKA, IN inhibitor L-708,906[25] or RNase H inhibitor[26]), 8-hydroxyquinoline-7-carboxamide[27] (among the first IN inhibitors in clinical trials, L-870,810 and L-870,812), 6-hydroxy-5-oxopyrimidinecarboxamide (raltegravir, the first FDA-approved IN inhibitor),[28] 2-hydroxyisoquinoline-1,3(2*H*,4*H*)-dione (RNase H inhibitor),[29] hydroxytropolones (among the first designed inhibitors of both IN and RNase H),[30,31] and madurahydroxylactone derivatives.[32]

The ability of such inhibitors to bind two divalent ions (at least partially) has been evidenced by us and others in the case of the DKA family.[33−35] Moreover, analysis of the drug-induced IN mutations led to the conclusion that these compounds inhibit viral replication by sequestering magnesium cations of the catalytic IN core.

Compared to the plethora of IN inhibitors, there are few examples of RNase H inhibitors, and to the best of our knowledge, none of them has revealed exceptional antiviral activities except for a series of compounds patented by Merck (see Scheme 1).[5,6] There is no firm physicochemical evidence that they complex magnesium cations within the RNase H catalytic center. However, RNase H cocrystallized with 2-hydroxyisoquinoline-1,3(2*H*,4*H*)-dione in the presence of manganese cations was reported in 2006.[36]

dx.doi.org/10.1021/jm1014692 |*J. Med. Chem.* 2011, 54, 1812–1824

Scheme 2. Structures of the Tested Compounds

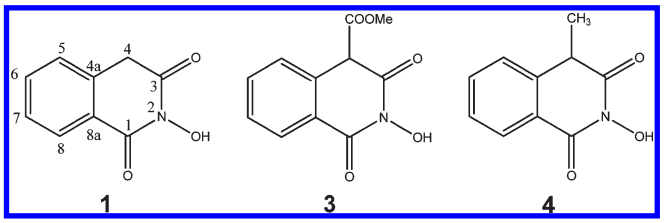

Starting from the pioneering work of Klumpp et al.,[29] we anticipated that 2-hydroxyisoquinoline-1,3(2*H*,4*H*)-dione **1** may be an ideal platform to design new RNase H and/or IN inhibitors depending on the substitution of this scaffold. For this purpose, we synthesized a series of substituted 2-hydroxyisoquinoline-1,3(2*H*,4*H*)-diones in order to study their ability to bind divalent ions in connection with their biological properties.[37,38]

In the present work, we investigate the interaction of 2-hydroxyisoquinoline-1,3(2*H*,4*H*)-dione **1** with two divalent cations (Mg^{2+} and Mn^{2+}). Depending on the nature of the cation, we used different spectroscopic methods: UV−vis spectroscopy to determine the stoichiometry of the complexes and their stability constants, IR spectroscopy, ^{1}H and ^{13}C NMR (for Mg^{2+}), and ESR (for Mn^{2+}) to determine their structures both in solid state and in solution. In order to evaluate the impact of a substitution at position 4, we also synthesized two analogues of **1**: one bearing an electron-withdrawing group (2-hydroxy-4-methoxycarbonylisoquinoline-1,3(2*H*,4*H*)-dione **3**) and the other bearing an electron-donating moiety (2-hydroxy-4-methylisoquinoline-1,3(2*H*,4*H*)-dione **4**) (Scheme 2). Their tautomeric forms in solution, as well as the stoichiometries and stability constants of their magnesium complexes, were related to their antiintegrase, antiRNase H, and antiviral activities together with those of **2**, the synthesized Mg^{2+} complex of **1**.

RESULTS

UV−Vis Spectroscopy—Stoichiometries and Stability Constants. The interaction of ligand **1** with magnesium cations was previously studied.[37] The stoichiometry (M/L) was found to be 1:1, and the value of K_s was 3.0×10^4 mol·L^{-1}. The elemental data obtained with the synthesized Mg^{2+} complex **2**, $[Mg(L)(H_2O)_4]$ (Scheme 3), were in perfect accordance with this stoichiometry, and its UV−vis spectrum fully superimposed on that obtained from equimolar mixtures of ligand and magnesium acetate at the same concentration. For compound **3** (Figure 1), the stoichiometry and stability constant were found to be 1:1 and $4.3 \pm 0.8\ 0 \times 10^3$ mol·L^{-1}, respectively. Compound **4** (Figure 2) interestingly displayed two stoichiometries, 1:1 (minor) and 1:2 (major), with respective K_s values of $2.0 \pm 0.9 \times 10^5$ mol·L^{-1} and $4.7 \pm 0.5 \times 10^7$ mol^2·L^{-2}.

In the case of Mn^{2+}, after 4 min of incubation of ligand **1** and Mn^{2+} solutions, UV spectra were recorded and the stoichiometry was found to be 1:2 and K_s was 8.0×10^7 mol^2·L^{-2}. After a longer time, the UV spectra of the solution still underwent strong modifications, but stoichiometry calculations gave the same result. The same UV spectra were obtained by mixing 2 equiv of the ligand **1** with manganese(III) acetate.

^{1}H and ^{13}C NMR Studies of the Ligands and Their Magnesium Complexes. Prior to magnesium cation complexation studies, a glance at the ^{1}H and ^{13}C NMR ligand spectra led us to have further insight into their structural features. Whereas **1** was exclusively obtained as its keto form, **3** and **4** were found to exist as mixtures of keto and enol forms with close keto to enol ratios of 55:45 and 60:40, respectively. Distinction between these two forms was based upon the H_4 and C_4 signals, and we could

Scheme 3. Structure of the Magnesium Complex 2

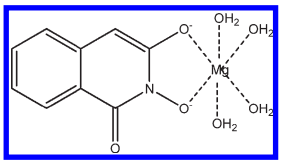

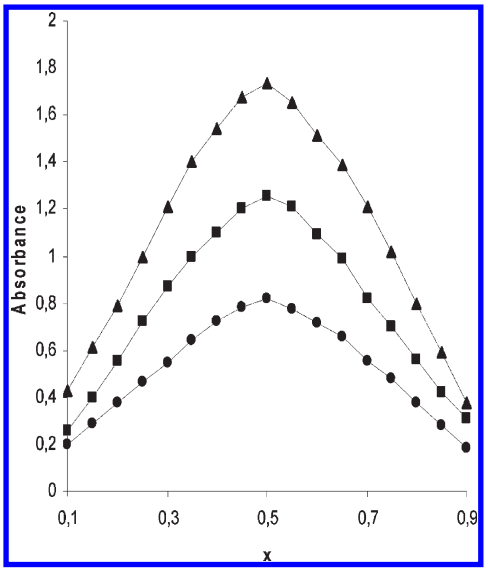

Figure 1. Job plots of **3** with Mg^{2+}: (●) 5×10^{-4} M and λ = 365.5 nm; (■) 8×10^{-4} M and λ = 302.5 nm; (▲) 8×10^{-4} M and λ = 365.5 nm.

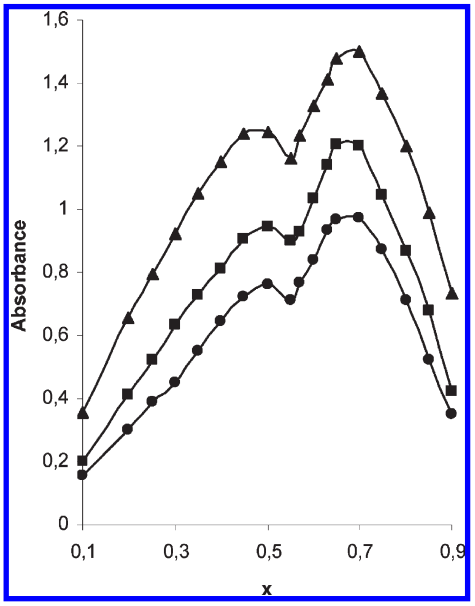

Figure 2. Job plots of **4** with Mg^{2+}: (●) 5×10^{-4} M and λ = 365.5 nm; (■) 8×10^{-4} M and λ = 302.5 nm; (▲) 8×10^{-4} M and λ = 365.5 nm.

dx.doi.org/10.1021/jm1014692 |*J. Med. Chem.* 2011, 54, 1812–1824

Scheme 4. Possible Tautomeric Forms of 3 and 4

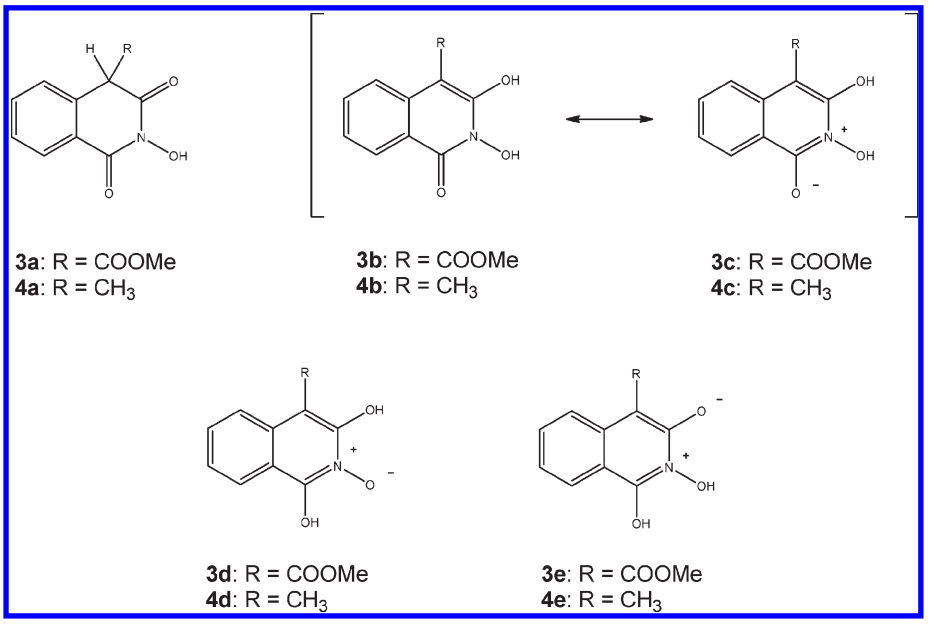

unambiguously establish the keto forms of **1**, **3**, and **4**. However, we had strong doubts about the exact canonical form of the other observed tautomer for **3** and **4**, arising from the set of chemical shifts attributed to the carbonyl carbons. The carbonyl carbons of **3** shifted from 161.0 ppm and 163.3 ppm for the keto form to 158.3 ppm and 161.0 ppm for the enol form, whereas, in the case of **4**, they shifted from 161.3 ppm and 170.1 ppm for the keto form to 146.7 ppm and 152.4 ppm for the enol form. Curiously, the substitution in position 4 had no effect on the chemical shift of carbon C_4 (83.7 ppm for **3**, 84.0 ppm for **4**, and 84.4 ppm for **2** (the magnesium complex of **1**)). These spectacularly high field shifts of the carbonyl signals led us to suspect aromatization of the enol form of **4**. Scheme 4 depicts the possible tautomeric states (ketonic, enolic, or aromatized) of **3** and **4**. In an attempt to solve this problem, we undertook to calculate the theoretical ^{13}C chemical shifts for the different possible tautomers.

Among magnetic shielding tensors calculation methods, the gauge invariant atomic orbitals (GIAO)[39] are currently the method of choice.[40] Regarding the theory level, density functional theory (DFT) has emerged as a good option, since it provides acceptable levels of accuracy at relatively low computational cost.[41,42]

Compounds **3** and **4** have four tautomeric forms each, which were all examined: a keto form **a**, an enolic form represented by two different resonance structures in the calculations (**b**/**c**), and two different aromatic forms **d** and **e**. The lowest energy conformers were first identified using a systematic pseudo-Monte Carlo search and the Merck molecular force field when applicable. The geometry of the selected conformers was pre-optimized at the AM1 level and further optimized at the B3LYP/6-31G(d) level. Gas phase GIAO ^{13}C NMR calculations were then carried out on the minimized structures at the B3LYP/6-311G+(d,p) level. Calculations were carried out using the Gaussian 03 package.[43]

$$\delta_{\text{calc}}{}^{x} = \sigma_{\text{ref}} - \sigma_x + \delta_{\text{ref}} \quad (1)$$

Chemical shifts were calculated according to eq 1, where σ_{ref} and σ_x are the NMR isotropic magnetic shielding values calculated at the same level of theory for the reference compound and the nucleus x of interest, respectively, and δ_{ref} is the experimental chemical shift of the reference compound. Considering that most carbons in the structures are sp^2-hybridized and that TMS has previously been shown to be an inappropriate standard in ^{13}C GIAO calculations for sp^2-hybridized carbons,[44−47] benzene was chosen as reference.

As shown in Table 1, the computed GIAO NMR chemical shifts for the keto forms **3a** and **4a** are in high accordance with experimental data, therefore validating this approach. As far as the second tautomer observed experimentally is concerned, carbons C_4 and, more surprisingly, C_1 are highly shielded when compared to the keto forms, exhibiting chemical shifts situated in the aromatic region and making it particularly difficult to elucidate whether it is enolic or aromatic. Although assignment of the second forms was less obvious from direct interpretation of the experimental spectra, the results obtained from this computational study strongly indicate that the second observed tautomer in each case corresponds to enols **3b**/**3c** and **4b**/**4c**. In addition to overall statistical values, there are two carbons that obviously discriminate between enolic and aromatic forms, namely C_4 and C_{8a}. The deviation between experimental and computed chemical shifts is well above 10 ppm in the case of aromatic forms **d** and **e**, ruling them out. However, predictions for the enolic form **b**/**c** are a lot more accurate for these two carbons as well as for the rest of the structure.

The complexation of ligand **1** with magnesium cations was previously investigated.[37] Briefly, in the absence of cation, the ^1H NMR spectrum of **1** presents five signals: a singlet at 4.26 ppm (2H, H_4), three aromatic signals at 7.37−7.52 ppm (H_7 and H_5), 7.70 ppm (H_6), and 8.03 ppm (H_8), and a broadened singlet at 10.4 ppm (OH). In the presence of 0.1−1.0 equiv of magnesium acetate, the singlets at 4.26 and 10.4 ppm progressively disappear and a singlet at 5.55 ppm is observed. For 1 equiv of magnesium acetate, four signals are observed at 5.55 ppm (1H, H_4), 6.83 ppm (H_6), 7.18 ppm (H_5 and H_7), and 7.80 ppm (H_8). The ^1H NMR spectrum of **1** in the presence of 1 equiv of magnesium acetate was in perfect

dx.doi.org/10.1021/jm1014692 |J. Med. Chem. 2011, 54, 1812–1824

Table 1. Analysis of the Differences in ^{13}C Chemical Shift between B3LYP/6-311G+(d,p) GIAO NMR Predictions and Experimental Results in d_6-DMSO for the Possible Tautomers of 3 and 4

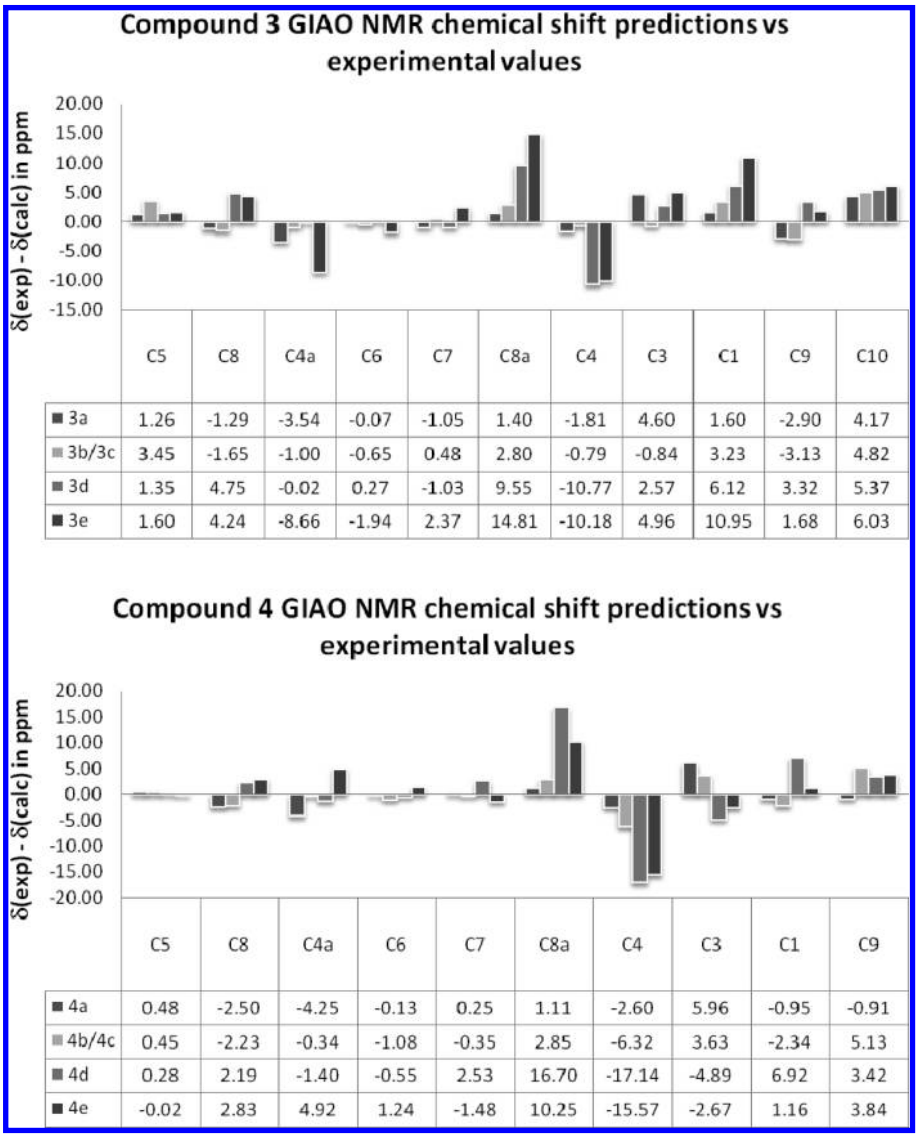

	C5	C8	C4a	C6	C7	C8a	C4	C3	C1	C9	C10
3a	1.26	-1.29	-3.54	-0.07	-1.05	1.40	-1.81	4.60	1.60	-2.90	4.17
3b/3c	3.45	-1.65	-1.00	-0.65	0.48	2.80	-0.79	-0.84	3.23	-3.13	4.82
3d	1.35	4.75	-0.02	0.27	-1.03	9.55	-10.77	2.57	6.12	3.32	5.37
3e	1.60	4.24	-8.66	-1.94	2.37	14.81	-10.18	4.96	10.95	1.68	6.03

	C5	C8	C4a	C6	C7	C8a	C4	C3	C1	C9
4a	0.48	-2.50	-4.25	-0.13	0.25	1.11	-2.60	5.96	-0.95	-0.91
4b/4c	0.45	-2.23	-0.34	-1.08	-0.35	2.85	-6.32	3.63	-2.34	5.13
4d	0.28	2.19	-1.40	-0.55	2.53	16.70	-17.14	-4.89	6.92	3.42
4e	-0.02	2.83	4.92	1.24	-1.48	10.25	-15.57	-2.67	1.16	3.84

accordance with that of the newly synthesized solid complex **2** at the same concentration and the observed peak of water (3.3 ppm) on the ^1H NMR spectrum of **2** integrated exactly for eight protons according to the elemental formula, $[Mg(L)(H_2O)_4]$ (these measurements were repeated three times with three different synthetic batches).

Additionally, three other series of experiments were carried out: instead of magnesium acetate, we added 2 equiv of sodium acetate. A quite different spectrum was then observed with five signals at 5.15 ppm (1H, H_4), 6.60 ppm (H_7), 6.95 ppm (H_8), 7.10 ppm (H_6), and 7.75 ppm (H_5). The addition of 2 equiv of sodium hydroxide gave a similar result whereas the addition of magnesium chloride did not rapidly modify the initial spectrum. Two weeks were needed to observe the appearance of complexation.

In the absence of complexation, the ^{13}C NMR spectrum of ligand **1** presents nine signals at 37.6 ppm (C_4), 125.6 (C_{8a}), 125.8, 126.5, 128.4, 131.8, and 135.7 (C_{4a}) ppm (aromatic carbons) and 161.3 and 166.0 ppm (carbonyl carbons). After magnesium complexation (1 equiv of magnesium acetate), the signal at 37.6 ppm disappears and a new signal at 84.4 ppm (C_4) is observed, the aromatic signals moderately shift (113.3 (C_{8a}), 117.8, 122.7, 125.4, 129.2, and 137.8 (C_{4a}) ppm), and the carbonyl carbon signals shift to high field (157.7 and 158.6 ppm). A similar ^{13}C NMR spectrum was obtained for the solid complex **2**.

IR Study of the Ligand 1 and Its Complex 2. The spectrum of **2** presented a large band at 3369−3434 cm^{-1}, which is absent in the IR spectrum of **1**, confirming the presence of molecules of water in the sphere of coordination of complex **2.** The two vibration bands (1723 and 1666 cm^{-1}) characteristic of the carbonyl bonds of **1** shifted to 1626 and 1551 cm^{-1} in complex **2**, and the vibration band at 2926−2920 cm^{-1} (methylene CH bonds of **1**) disappeared. These results attest the formation of an enolate upon magnesium complexation.

ESR Study of the Mn^{2+} Complex of 1. The Mn^{2+} ESR spectra were recorded for different ratios Mn^{2+}/ligand

dx.doi.org/10.1021/jm1014692 |J. Med. Chem. 2011, 54, 1812–1824

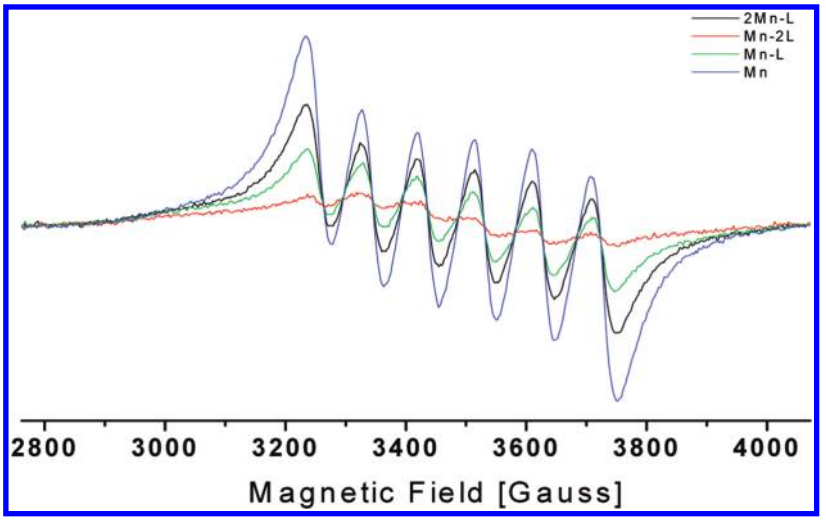

Figure 3. ESR spectra of a 1 mM methanolic solution of $Mn(OAc)_2$ (blue) with 0.5 (black), 1.0 (green), and 2.0 (red) equiv of **1**.

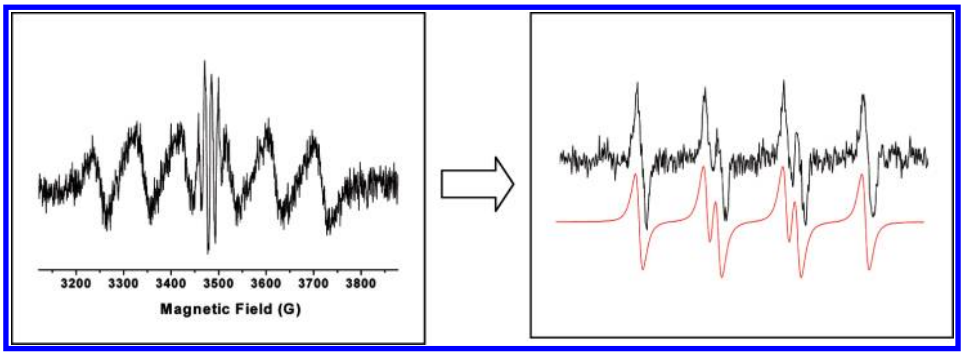

Figure 4. (left) ESR spectrum of a solution in DMSO of $Mn(OAc)_2$ and 2 equiv of **1** in the presence of DMPO. (right) Experimental and simulated ESR spectra of DMPO-OOH°.

in methanol. The characteristic six-line signal of Mn^{2+} (Landé factor g = 2.0153, a(iso) = 94.31 G) disappeared for a ratio of one Mn^{2+} for two ligands (Figure 3). Since this result indicated that Mn^{2+} is probably oxidized to silent oxidized forms of manganese, we therefore carried out the same experiment in DMSO in the presence of DMPO.

A new six-line signal superimposed on the Mn^{2+} signal (Figure 4) that is characteristic of the adduct DMPO-OOH (a_N = 14.15 G and a_H = 11.3 G).

Anti-IN, anti-RNase H, and Antiviral Properties. The inhibitory potency of 2-hydroxyisoquinoline-1,3(2*H*,4*H*)-diones **1**, **3**, and **4** and magnesium complex **2** was evaluated on HIV-1 integrase (Figure 5) and HIV-1 reverse transcriptase ribonuclease H and polymerase functions (Figure 6).Their effect on HIV-1 replication was also evaluated on MT-4 cells. Results are reported in Table 2; the values determined for raltegravir[28] and the best published Merck's RNase H inhibitor[5] are included for the purpose of comparison. **1** and its magnesium complex **2** revealed very similar inhibitory activities on both integrase (IC_{50} around 5.2 μM) and RNase H (IC_{50} around 4.5 μM).

In order to replicate, HIV needs to establish itself as a provirus in the host. Therefore, integrase promotes the integration of the cDNA copy of the viral RNA genome into the host chromatin. For this purpose, IN needs to catalyze two reactions, namely the 3′-processing reaction, producing recessed DNA ends by endonucleolytic cleavage of the conserved CA dinucleotide at the 3′-terminus of the viral DNA, and the strand transfer reaction resulting in the insertion of both recessed viral DNA ends into the host-cell chromosome. State of the art ELISA based assays allow evaluation of the overall enzymatic activity (3′-processing and strand transfer) of integrase inhibitors. Using preprocessed substrates, the strand transfer reaction can be decoupled from the 3′-processing reaction. To date, the only integrase inhibitor approved for its use in the clinic, Raltegravir, inhibits the strand transfer reaction. Compounds **1**, **2**, and **3** inhibit the integrase reaction in both assays with nearly identical IC_{50} (Table 2), pointing out that the integrase inhibition is probably due to strand transfer inhibition. The substitutions at position 4 led to contrasted results. A methoxycarbonyl group conferred to **3** a remarkable RNase H inhibitory activity (IC_{50} = 61 nM) but did not strongly modify the anti-integrase activity of **1**. Conversely, a methyl group had a negative effect on the inhibition of RNase H (IC_{50} = 38.8 μM). This excellent RNase H inhibitory activity conferred to **3** an appreciable antiviral activity with an EC_{50} of 13.4 μM and a therapeutic index of 4.5, whereas the other compounds exhibited limiting cytotoxicities. In order to gain insight into the mechanism of action of **3** and in spite of a low therapeutic index, a cross-resistance profile of **3** was measured. In total, three different strains resistant against integrase and RT inhibitors were included. For integrase, two different kinds of

inhibitors have been described so far. Strand transfer inhibitors, such as Raltegravir, inhibit the enzymatic reaction of integrase directly by binding to the catalytic core of integrase and displacing the single stranded processed substrate[15] of the viral DNA. LEDGINs, on the other hand, are experimental drugs inhibiting the viral integration in cell culture by binding on an allosteric site on integrase and therefore displacing the cellular cofactor of integration LEDGF/p75.[48] Interestingly, **3** does not show any cross-resistance with both types of inhibitors (see Table 3, resistance strains A128T and G140S/Q148H[49]), clearly indicating the novel mechanism of action of compound **3** in comparison with known integration inhibitors. The same finding is observed for the non-nucleotide reverse transcriptase inhibitors[50] (NNRTI) (see Table 3 A17R). Hence, compound **3** represents a novel strategy for inhibiting HIV replication in cell culture.

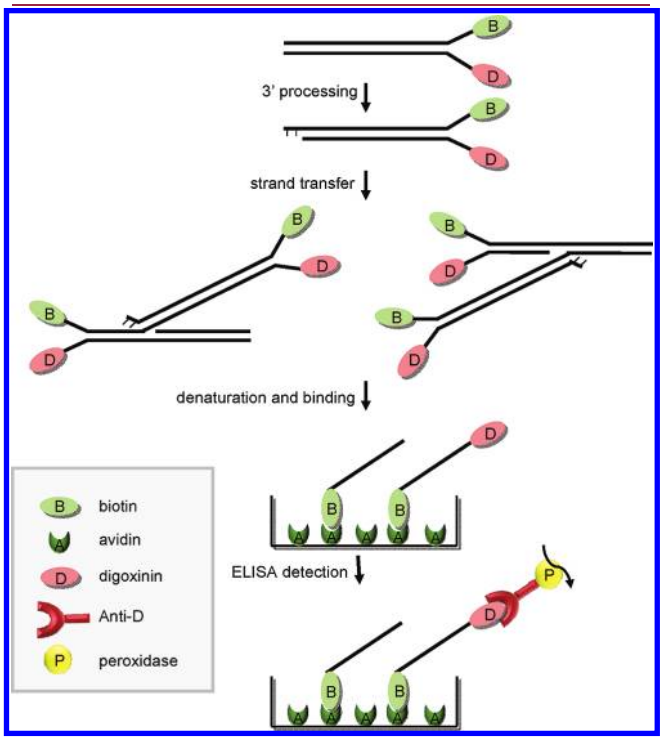

Figure 5. Schematic outline of a standard ELISA assay as described in detail in the Methods section. Oligodeoxynucleotides resembling the viral 5′ LTR sequence are labeled with biotin (B) and digoxigenin (D) in the complementary strand. After 3′-processing and strand transfer, the reaction products are denatured and bound to streptavidine coated (A) microtiter plates. The *overall enzymatic activity* is analyzed by detecting the digoxigenin label with a specific antibody fused to peroxidase. In order to analyze the *strand transfer enzymatic activity*, the first step is omitted and a preprocessed substrate is used.

DISCUSSION

2-Hydroxyisoquinoline-1,3(2*H*,4*H*)-dione **1** easily formed complexes with divalent cations with 1:1 and 1:2 stoichiometries for Mg^{2+} and Mn^{2+}, respectively. These stoichiometries were established using UV−vis and resonance spectroscopies in solution (^{1}H NMR for Mg^{2+} and ESR for Mn^{2+}). In the case of Mg^{2+}, complex **2** was also synthesized and its NMR data were similar to those obtained after mixing solutions of ligand and magnesium acetate at the same concentration. Unfortunately, this isolated magnesium complex was amorphous and its crystallographic structure could not be obtained.

IR and NMR data confirmed the facile enolization of the ligand when complexed both in solution (NMR) and at the solid state (IR). Since the pK_a of the proton of the hydroxyl imide group is about 8,[51] we reasonably assume that the ligand is bianionic in the presence of magnesium cations. The coordination sphere is completed with four molecules of water that can be characterized by IR and quantified from the ^{1}H NMR spectrum of the magnesium complex in a solution of dry DMSO-d_6. We propose the structure given in Scheme 3 for the solid magnesium complex **2**.

Interestingly, ligand **1** also complexed Mn^{2+} cations. Due to the instability (in the first few minutes of the reaction) of the UV−vis spectra, we decided to measure the stoichiometry at a fixed short time (4 min) and after a longer time (30 min) when the spectra did not evolve any more. In both cases, the stoichiometry was 1:2. This stoichiometry was already observed for 2,3-dihydroxyquinoline.[52] However, the ESR study suggested that Mn^{2+} is oxidized. The six-line signal characteristic of Mn^{2+} disappeared for exactly 2 equiv of ligand. We suppose that a

Table 2. Inhibition of HIV-1 IN and RT RNase H Activities, Antiviral Activity, and Cytotoxicity of Compounds 1−4 (IC_{50} in μM)

			IN activity		activity in MT-4 cells	
compd	RNase H activity[a] of RT, IC_{50}	polymerase activity[b] of RT, IC_{50}	overall[c] IC_{50}	ST[d] IC_{50}	HIV-1[e] EC_{50}	cytotoxicity[f] CC_{50}
1	5.91 ± 2.44	>50	6.32 ± 2.61	7.91 ± 2.71	>27.05	27.05
2	3.01 ± 1.25	NT	4.11 ± 1.85	2.89 ± 2.27	>69.13	69.13
3	0.061 ± 0. 005	>50	4.77 ± 0.58	4.90 ± 0.1.7	13.44 ± 4.4	60.85 ± 2.85
4	38.8	>50	3.30 ± 1.73	NT	>250	>250
Raltegravir[28]	>25	>100		0.002−0.007	0.013 ± 0.0005	>18
Merck's RNase H inhibitor[5,6]	0.045 ± 0. 02[g]	13 ± 1.3[h]		24	0.19 ± 0. 12[i]	3.3 ± 2.3[j]

[a] Concentration required to inhibit by 50% the in vitro RNase H activity of HIV-1 RT. Values are means ± standard deviations from at least three independent experiments. [b] Concentration required to inhibit by 50% the in vitro polymerase activity of HIV-1 RT. Values are means ± standard deviations from at least three independent experiments. [c] Concentration required to inhibit by 50% the in vitro overall integrase activity. Values are means ± standard deviations from at least three independent experiments. [d] Concentration required to inhibit by 50% the in vitro strand transfer integrase activity. Values are means ± standard deviations from at least three independent experiments. [e] Effective concentration required to reduce the HIV-1-induced cytopathic effect by 50% in MT-4 cells. Values are means ± standard deviations from at least three independent experiments. [f] Cytotoxic concentration required to reduce MT-4 cell viability by 50%. Values are means ± standard deviations from at least three independent experiments. [g] RNase H assay using wild-type HIV-1-RT. [h] Polymerase assay using D443N HIV-1-RT. [i] HIV-1 HXB2 single cycle viral replication assay in HeLa P4-2 cells. [j] CC_{50} = concentration for 50% cytotoxic response using Alamar Blue indicator in HeLa P4-2 cells

dx.doi.org/10.1021/jm1014692 |*J. Med. Chem.* 2011, 54, 1812–1824

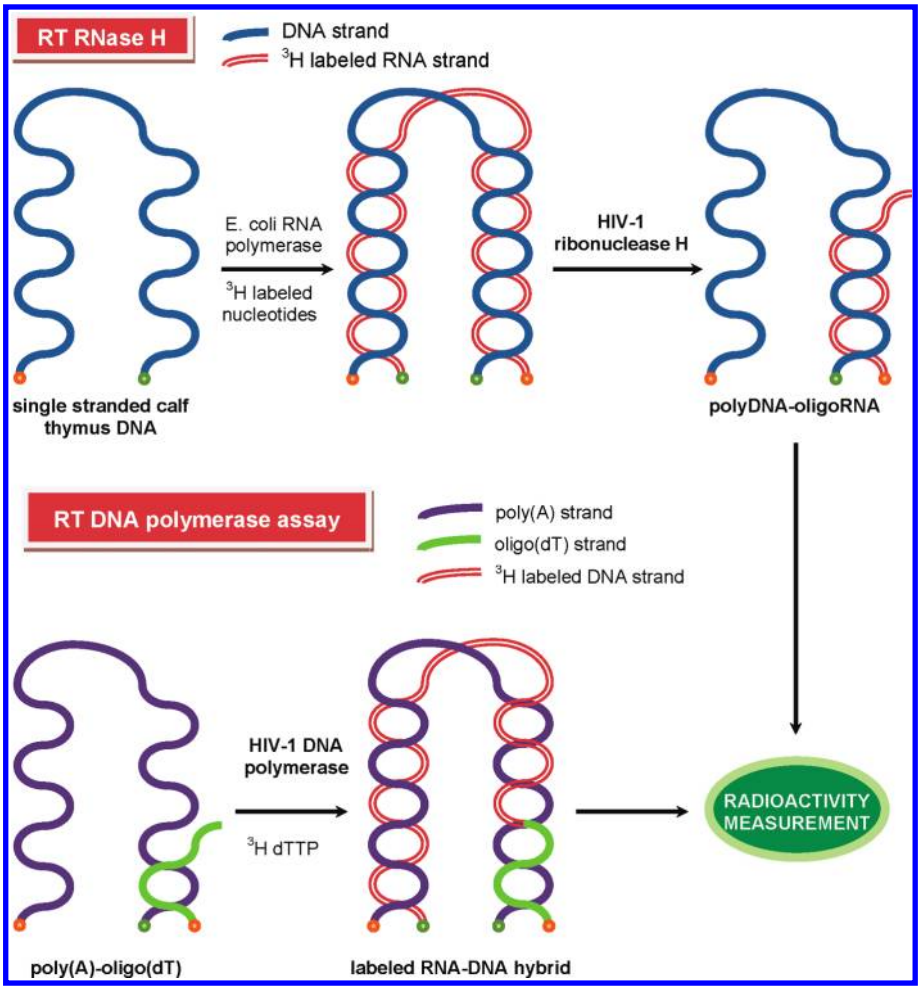

Figure 6. Schematic outline of the HIV-1 reverse transcriptase RNase H and the DNA polymerase assays.

Table 3. Reduced Susceptibilities of Resistant HIV Strains to Compound 3 and Reference Compounds

		viral target			
		integrase		reverse transcriptase	
resistance	virus strain[a]	compound **3**	raltegravir	efavirenz	AzaT
LEDGIN[b]	IN-A128T	2[c]	1	1	1
raltegravir	IN-G140S/ Q148H[d]	1	>400	1	1
efavirenz	RT-A17R IIIB[e]	1	1	17	1

[a] Viral strain selected to be resistant against the drugs mentioned in the first column of the table. [b] A strain was selected to be resistant against the LEDGINs.[48] [c] Fold resistance in comparison with the respective WT-strain of HIV-1. [d] Raltegravir resistant strains[49] (and references within). [e] HIV-1 strain resistant to NNRTIs.[50]

L_2Mn^{2+} complex is formed at first. Manganese then rapidly oxidizes in the presence of dissolved oxygen to form a $(L_2MnO_2)^{2+}$ complex silent in ESR (Scheme 5) that decomposes into a stable L_2Mn^{3+} complex, leading to the simultaneous production of superoxide anion. Hydroxysalen manganese complexes have previously been identified as superoxide generators.[53] In the presence of the spin trap DMPO, a new six-line signal characteristic of the trapping of superoxide anion was observed. This observation is of particular interest, since enzymatic assays with integrase and RNase H sometimes use Mn^{2+} as cofactor. Moreover, cocrystallization of an enzyme and its inhibitor with divalent metallic cations is problematic if this cation is implicated in a redox process.

As previously shown in the case of diketoacids[35] and rosmarinic acid,[54] Mg^{2+} complex **2** exhibits a slightly better inhibitory activity on enzymes than **1**. The stability constant is sufficiently high to assume that ligand **1** binds magnesium cations during the inhibition assays. This is supported by the very close IC_{50}'s of ligand **1** and its magnesium complex **2** on both enzymes (Table 2). Integrase inhibition is probably due to strand transfer inhibition, as shown when this specific enzymatic activity is studied. Antiviral activities could not be evaluated due to limiting cytotoxicities. Here again, **2** was found to be three times less toxic than **1**.

Substitution at position 4 had particular implications on enzymatic activities. **3** and **4** revealed antiintegrase activities similar to that of **1**. On the contrary, the effect on RNase H activity was much more contrasted. Whereas an electron-donating methyl group (compound **4**) strongly decreased RNase H inhibition, introduction of an electron-withdrawing methoxycarbonyl moiety (compound **3**) revealed a major influence on this activity (IC_{50} = 61 nM) and places **3** among the best RNase H inhibitors ever reported (as a point of reference, Merck's RNase

dx.doi.org/10.1021/jm1014692 |J. Med. Chem. 2011, 54, 1812–1824

Scheme 5. Superoxide Anion Release from the Manganese Complex of 1

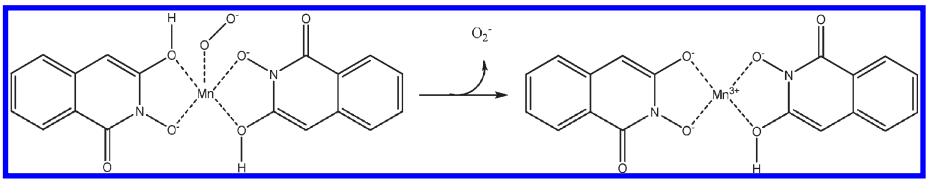

H inhibitor has an IC_{50} of 45 nM;[5,6] see the biological data reported in Table 2). This may be due to resonance stabilization of the corresponding enolate, the formation of which is required for metal chelation. Indeed, density functional relative energy calculations of the different tautomers at the B3LYP/6-311G+(d,p) level indicate that the **3b**/**3c** enol form is more stable than the keto form **3a** by nearly 6 kcal·mol^{-1} (see the Supporting Information). This fact seems to have a great influence on the biological activities of **3**, particularly RNase H inhibition. On the other hand, the presence of an inductive electron-donating methyl moiety on C_4 favors the keto form of **4** and increases the acidic proton's pK_a. Compound **4** might then not be able to easily recruit divalent metal ions upon entering the active site of RNase H. All compounds presented a 1:1 cation chelating stoichiometry in solution except for compound **4**, which could also predominantly complex magnesium cations in a 1:2 manner. At this stage of the study, it would be hazardous to establish any relationship between complexation stoichiometries in solution and enzymatic inhibitions. The series must be developed to a larger extent in order to try to achieve this goal.

None of the tested compound inhibited the polymerase function of RT at concentrations up to 50 μM, leading to a selectivity ratio (Pol/RNase H) of >820 for **3**. Interestingly, only compound **3** was effective on viral replication among the series. In order to have more information on the mechanism of action of **3**, we measured its antireplication potency on HIV-1 resistant strains. The first two strains present mutation on IN. Mutation A128T has been previously isolated in one of our laboratories from resistance to a new inhibitor of the interaction IN/LEDGF,[48] and the double mutant G140S/Q148H corresponds to the most resistant strain to raltegravir.[49] The third selected strain A17R IIIB is one of the classical viral strain resistant to NNRTI (efavirenz, for example).[50] The AzaT resistance strain (RTMC) is based on a HXB2D. Unfortunately, **3** is not active enough to be able to inhibit this strain; therefore, we could not include the AzaT resistant strain in the analysis. Cross-resistance results reported in Table 3 show that the antiviral activity of **3** is probably related to its action on the ribonuclease H function of reverse transcriptase. Further investigations, such as time-of-addition experiments, are needed to confirm or invalidate this hypothesis. Among the reasons that might account for the contrast in activity between enzymatic and cellular assays are insufficient intrinsic potency, low cell permeability, or high protein binding. Starting from this remarkable hit, further experiments are underway in our laboratories to develop this novel family of selective inhibitors of RT RNase H function, optimize its pharmacokinetic properties, and increase its antiviral potency.

CONCLUSION

We demonstrated in this article that 2-hydroxyisoquinoline-1,3(2*H*,4*H*)-dione (**1**) and methyl 2-hydroxy-1,3-dioxo-1,2,3,4-tetrahydroisoquinoline-4-carboxylate (**3**) efficiently bind magnesium cations in a 1:1 stoichiometry. At first sight, this result seems in opposition to the hypothetic binding of two divalent magnesium ions proposed by Klumpp et al.[29] However, it only reflects the best metal chelating site of the ligand in solution and in the absence of any protein and does not exclude the possibility that it may also interact with a second metal ion by a perfect fit into the catalytic active site of the enzyme, which may be illustrated by the orientation of raltegravir in the IN active site of PFV.[15]

In this study, 2-hydroxyisoquinoline-1,3(2*H*,4*H*)-dione is once again revealed as a formidable scaffold for the design of integrase and/or ribonuclease H inhibitors. We have shown in a first article[37] that placing benzamide or phenacetamide groups at position 7 strongly improves the anti-IN activity. Herein the two first examples of substitution at position 4 revealed contrasted results, and a strong inhibitor of RNase H was evidenced. Very recently, we have shown that the selectivity of this scaffold can be optimized for integrase activity by substituting position 4 with lipophilic alkyl moieties.[38] However, due to a lack of activity on viral replication, further optimization of this scaffold is needed for the development of a suitable new class of antiretroviral agents acting as selective inhibitors of IN or RNase H. We naturally keep in mind that an ester group is usually unattractive, mainly due to possible metabolic instability. These studies will be reported in due course.

EXPERIMENTAL SECTION

Materials and Methods. All reagents and solvents were purchased from Aldrich-Chimie (Saint-Quentin-Fallavier, France), were ACS reagent grade, and were used as provided. NMR spectra were obtained on an AC 300 Bruker spectrometer in the appropriate solvent with TMS as an internal reference. Chemical shifts are reported in δ units (parts per million) and are assigned as singlets (s), doublets (d), doublets of doublets (dd), triplets (t), quartets (q), quintets (quin), sextuplets (sext), multiplets (m), and broad signals (bs).

Melting points were obtained on a Reichert Thermopan melting point apparatus, equipped with a microscope, and are uncorrected.

Mass spectra were recorded on a Thermo-Finnigan PolarisQ mass spectrometer (70 eV, Electronic Impact). Elemental analyses were performed by CNRS laboratories (Vernaison).

The UV−vis study was carried out on a JASCO V-530 UV/vis spectrometer equipped with a water thermostable 4-position turret cell holder (MHT-344).

Infrared spectra were obtained on a Perkin-Elmer 881 spectrometer on KBr paths.

X-band ESR spectra were obtained with a Bruker Elexsys 580 spectrometer operating at 100 kHz modulation frequency at room temperature (20 °C). The *g* factor measurements were related to the "strong pitch", $g = 2.0028$.

Elemental analyses were performed by CNRS laboratories (Vernaison) and were within 0.4% of the theoretical values.

Chemistry. *2-Hydroxyisoquinoline-1,3(2H,4H)-dione LH_2 (**1**) and Its Magnesium Complex $[Mg(L)(H_2O)_4]$ (**2**).* The ligand **1** was synthesized in a two step procedure[37] from commercially available homophthalic anhydride. Keto form (100%): orange solid; yield 86%; mp 199 °C (butanone); ^{1}H NMR (DMSO-d_6) δ 4.26 (s, 2H, H_4), 7.37−7.52 (m, 2H, H_7, H_5), 7.70 (td, 1H, ^3J = 7.6 Hz, ^4J = 1.5 Hz, H_6), 8.03 (dd, 1H, ^3J = 7.6 Hz, ^4J = 1.5 Hz, H_8), 10.4 (s, 1H, OH); ^{13}C NMR (DMSO-d_6) δ 37.6 (C_4), 125.6 (C_{8a}), 125.8 (C_7), 126.5 (C_8), 128.4 (C_5), 131.8 (C_6), 135.7 (C_{4a}), 161.3 (C_1), 166.0 (C_3); ESI-MS m/z 178 $(M + H)^+$; IR (cm^{-1}, KBr cells; b broad; m medium; w weak; s strong) 3300 (bm), 3188 (bm), 2926 (w), 2900 (w), 1725 (s), 1666 (s), 1608 (m), 1463 (m), 1431 (m), 1372 (m), 1263 (s), 1169 (m), 929 (m), 731 (m). $C_9H_7NO_3$: Calcd C 61.02, H 3.98, N 7.91; Found C 61.13, H 4.23, H 7.62.

The magnesium complex **2** was synthesized according to the procedure described by Sechi et al.[34] Enol form (100%): yield 80%; ^{1}H NMR (DMSO-d_6) δ 3.30 (bs, 8H, 4 H_2O), 5.55 (bs, 1H, H_4), 6.83 (td, 1H, ^3J = 7.6 Hz, ^4J = 1.5 Hz, H_6), 7.18−7.22 (m, 2H, H_7, H_5), 7.80 (dd, 1H, ^3J = 7.6 Hz, ^4J = 1.5 Hz, H_8); ^{13}C NMR (DMSO-d_6) δ 84.4 (C_4), 113.3 (C_{8a}), 117.8 (C_7), 122.7 (C_8), 125.4 (C_5), 129.2 (C_6), 137.8 (C_{4a}), 157.7 (C_1), 158.6 (C_3); ESI-MS m/z 390 (6%, $[^{26}Mg(L)(H_2O)_4 + DMSO + K]^+$), 388 (38%, $[^{24}Mg(L)(H_2O)_4 + DMSO + K]^+$), 374 (33%, $[^{26}Mg(L)(H_2O)_4 + DMSO + Na]^+$), 372 (100%, $[^{24}Mg(L)(H_2O)_4 + DMSO + Na]^+$); IR (cm^{-1}, KBr cells; b broad; m medium; w weak; s strong): 3375 (bs), 1630 (s), 1555 (s), 1522 (m), 1461 (m), 1364 (m), 1204 (w), 961 (m), 796 (w). $C_9H_{13}MgNO_7$: Calcd C 39.81, H 4.83, N 5.16; Found C 40.05, H 5.12, H 5.48.

*Methyl 2-Hydroxy-1,3-dioxo-1,2,3,4-tetrahydroisoquinoline-4-carboxylate (**3**).* Methyl 2-(benzyloxy)-1,3-dioxo-1,2,3,4-tetrahydroisoquinoline-4-carboxylate[55] (1.0 mmol) was dissolved in a minimum amount of CH_2Cl_2, and boron trichloride (1.0 M solution in CH_2Cl_2, 6.0 mL, 6.0 mmol) was added dropwise at room temperature. The solution was stirred for 1 h, and water (20 mL) was slowly added. After the mixture had been stirred for 5 min, the precipitate was filtered and the aqueous layer was extracted with ethyl acetate. Organic layers were dried over Na_2SO_4 and concentrated in vacuum. Organic residues and precipitate were gathered and triturated in anhydrous ether to give **3** as a white powder in 85% yield; mp 166−168 °C. Keto form (55%): ^{1}H NMR (DMSO-d_6) δ 3.71 (s, 3H, OCH_3), 5.47 (s, 1H, CH), 7.43 (dd, 1H, $^3J_{5-6}$ = 7.6 Hz, $^4J_{5-7}$ = 1.6 Hz, H_5), 7.60 (td, 1H, HAr, ^3J = 7.6 Hz, ^4J = 1.6 Hz), 7.72 (td, 1H, HAr, ^3J = 7.5 Hz, ^4J = 1.6 Hz), 8.10 (dd, 1H, $^3J_{8-7}$ = 7.6 Hz, $^4J_{8-6}$ = 1.5 Hz, H_8); ^{13}C NMR (DMSO-d_6) δ 52.9 (C_4), 54.0 (OCH_3), 124.7 (C_{8a}), 127.3 (C_7), 128.2 (C_8), 128.9 (C_5), 132.2 (C_{4a}), 134.2 (C_6), 161.0 (C_1), 163.3 (C_3), 167.5 (COO). Enol form (45%): ^{1}H NMR (DMSO-d_6) δ 4.00 (s, 3H, OCH_3), 7.38 (td, 1H, HAr, ^3J = 7.5 Hz, ^4J = 1.6 Hz), 7.72 (td, 1H, HAr, ^3J = 7.5 Hz, ^4J = 1.6 Hz), 8.20 (dd, 1H, $^3J_{5-6}$ = 7.5 Hz, $^4J_{5-7}$ = 1.6 Hz, H_5), 8.40 (dd, 1H, $^3J_{8-7}$ = 7.5 Hz, $^4J_{8-6}$ = 1.6 Hz, H_8); ^{13}C NMR (DMSO-d_6) δ 53.4 (OCH_3), 83.7 (C_4), 120.0 (C_{8a}), 123.9 (C_7), 127.6 (C_8), 127.9 (C_5), 132.8 (C_{4a}), 133.2 (C_6), 158.3 (C_1), 161.0 (C_3), 171.6 (COO); ESI-MS m/z 236 $(M + H)^+$. $C_9H_7NO_3$: Calcd C 56.17, H 3.86, N 5.96; Found C 55.99, H 3.78, N 6.12.

*2-Hydroxy-4-methylisoquinoline-1,3(2H,4H)-dione (**4**).* The synthesis of **4** has already been described.[38]

UV−Vis Spectroscopy—Stoichiometries and Stability Constants. The interaction of 2-hydroxyisoquinoline-1,3(2*H*,4*H*)-diones with divalent cations was studied in methanolic solution by mixing solutions of ligand (**1**, **3**, or **4**) and cation or after dissolution in methanol of the solid complex **2**.

The stoichiometries of the complexes were measured using the previously reported Job method.[37] Solutions of 2-hydroxyisoquinoline-1,3(2*H*,4*H*)-dione and metal acetate in methanol of the same concentration were prepared. The variation of the absorption was measured at 302.5 and 365.5 nm for solutions containing $(1 - x)$ mL of the acetate solution and x mL of ligand solution; the reference cuvettes contained x mL of ligand solution and $(1 - x)$ mL of methanol. pH was made constant by adding sodium acetate to the reference solution. By plotting the absorbance as a function of the molecular fraction of ligand, the maxima of the curves give the stoichiometries of the complexes.

For the determination of the stability constants, the same method was used with differently concentrated ligand and metal acetate solutions. K_d can be obtained using eq 2:

$$K_d = \frac{[M]^{m+n-1}p^{n-1}[(n+mp)x - n]^{m+n}}{m^{n-1}n^{m-1}(p-1)^{m+n-1}[n-(m+n)x]} \qquad (2)$$

where p = [L]/[M] ([M] being the concentration of the metal acetate and [L] the concentration of the ligand). In the case of Mn^{2+}, we observed variations of the absorbance during time and decided to record the spectra 4 and 30 min after mixing the two solutions.

*^{1}H and ^{13}C NMR Study—Stoichiometry and Structure of the Magnesium Complex of **1**.* The NMR study was carried out only on the complexation of **1** with Mg^{2+}, since Mn^{2+} is paramagnetic and induces a strong broadening and shifting of all the signals. In order to avoid a possible interference of rapid hydration of dry magnesium acetate, we used magnesium acetate tetrahydrate and controlled that water did not modify the spectrum of 2-hydroxyisoquinoline-1,3-dione. Water (6% v/v) was added to a 10^{-2} M solution of **1** in DMSO-d_6.

The complexation was studied by adding variable volumes of 10^{-2} M solutions of magnesium acetate and **1** in DMSO-d_6. Additionally, three other experiments were performed with 2 equiv of sodium acetate (in order to maintain the acetate concentration) and 2 equiv of sodium hydroxide or magnesium chloride.

*ESR Study of the Mn^{2+} Complex of **1**.* The Mn^{2+} ESR spectra were recorded for methanolic solutions of ligand and manganese acetate at different Mn^{2+}/ligand ratios. Spin trapping experiments were performed to detect reactive oxygen species produced upon variation of the redox state of manganese. DMSO was used as solvent, and 5,5′-dimethylpyrroline *N*-oxide (DMPO) provided the spin trapping agent.

Biology. *Integrase Inhibition.* To determine the susceptibility of the HIV-1 integrase enzyme to different compounds, we used an enzyme-linked immunosorbent assay. This assay uses an oligonucleotide substrate in which one oligo (5′-ACTGCTAGAGATTTTCCACACTGACTAAAAGGGTC-3′) is labeled with biotin on the 3′-end and in which the other oligo is labeled with digoxigenin at the 5′-end. For the overall integration assay, the second 5′-digoxigenin-labeled oligo is 5′-GACCCTTTTAGTCAGTGTGGAAAATCTCTAGCA**GT**-3′. The integrase was diluted in 750 mM NaCl, 10 mM Tris (pH 7.6), 10% glycerol, 1 mM β-mercaptoethanol, and 0.1 mg/mL bovine serum albumin. To perform the reaction, 4 μL of diluted integrase (corresponds to a concentration of WT integrase[56] of 1.6 μM) and 4 μL of annealed oligos (7 nM) were added in a final reaction volume of 40 μL containing 10 mM $MgCl_2$, 5 mM DTT, 20 mM HEPES (pH 7.5), 5% PEG, and 15% DMSO. The reaction was carried out for 1 h at 37 °C. These reactions were followed by an immunosorbent assay on avidin-coated plates.[57] Strand transfer assays were performed according to previously reported methods.[58]

RT Assays

(i) RNase H Assay. The substrate for RNase H activity was prepared as previously described.[59] *E. coli* RNA polymerase used single-stranded calf thymus DNA as a template to synthesize complementary ^{3}H-labeled RNA. For RNase H activity, recombinant HIV-1 RT[60] (4.5 pmol) was incubated with the appropriate compound for 10 min at 37 °C in 20 μL. The components of the incubation mixture were added to reach a final concentration of 50 mM Tris-HCl (pH 8.0), 10 mM dithiothreitol, 6 mM $MgCl_2$, 80 mM KCl, and the labeled nucleic acid duplex (20000 cpm) in a final volume of 50 μL. After incubation for 10 min at 37 °C, the

reaction was stopped by addition of 1 mL of cold 10% TCA containing 0.1 M sodium pyrophosphate, the acid-precipitable material was collected on nitrocellulose filters and washed, the radioactivity was determined, and the radioactivity released from the hybrid was determined by subtraction from the undigested hybrid control.

(ii) DNA Polymerase Assay. Recombinant RT was incubated with the appropriate compound for 10 min at 37 °C in 20 μL. Then incubation was carried out at 37 °C for 10 min. The reaction mixture contained, in a final volume of 0.05 mL, 50 mM Tris-HCl (pH 8.0), 5 mM $MgCl_2$, 10 mM dithiothreitol, 100 mM KCl, 20 μg/mL poly(A)-oligo(dT), 0.5 μCi of [^{3}H]dTTP (56 Ci/mmol), 20 μM dTTP, and enzyme. Reactions were stopped by the addition of 1 mL of 10% cold trichloroacetic acid with 0.1 M sodium pyrophosphate. The precipitate was filtered through a nitrocellulose membrane washed with 2% trichloroacetic acid and dried, and the radioactivity was determined.

In Vitro Anti-HIV and Drug Susceptibility Assays. The inhibitory effect of antiviral drugs on the HIV-1-induced cytopathic effect (CPE) in human lymphocyte MT-4 cell culture was determined by the MT-4/MTT assay.[61] This assay is based on the reduction of the yellow colored 3-(4,5-dimethylthiazol-2-yl)-2,5-diphenyltetrazolium bromide (MTT) by mitochondrial dehydrogenase of metabolically active cells to a blue formazan derivative, which can be measured spectrophotometrically. The 50% cell culture infective dose ($CCID_{50}$) of the HIV-1 (III_B) strain was determined by titration of the virus stock using MT-4 cells. For the drug susceptibility assays, MT-4 cells were infected with 100−300 $CCID_{50}$ of the virus stock in the presence of 5-fold serial dilutions of the antiviral drugs. The concentration of various compounds achieving 50% protection against the CPE of the different HIV strains, which is defined as the EC_{50}, was determined. In parallel, the 50% cytotoxic concentration (CC_{50}) was determined.

■ ASSOCIATED CONTENT

Supporting Information. Complete details of calculated ^{13}C nuclei magnetic shielding constants, experimental chemical shifts, and statistical values (coefficient of determination and mean absolute error of the different canonical forms of **3** and **4**, as well as computed relative energies). This material is available free of charge via the Internet at http://pubs.acs.org.

■ AUTHOR INFORMATION

Corresponding Author

*Telephone: +33 320 434 939. Fax: +33 320 336 309. E-mail: philippe.cotelle@univ-lille1.fr.

■ ACKNOWLEDGMENT

This work was financially supported by grants from la Région Nord Pas-de-Calais, le Centre National de la Recherche Scientifique (CNRS), l'Agence Nationale de la Recherche contre le Sida (ANRS), and the European Commission (LSHB-CT-2003-503480). The European TRIoH Consortium is gratefully acknowledged. The Mass Spectrometry facility used in this study was funded by the European Community (FEDER), the Région Nord-Pas de Calais (France), the CNRS, and the Université des Sciences et Technologies de Lille. We are grateful to Martine Michiels, Nam Joo Vanderveken, and Barbara Van Remoortel for excellent technical assistance.

■ ABBREVIATIONS USED

HIV-1, human immunodeficiency virus type 1; RT, reverse transcriptase; RNase H, ribonuclease H; IN, integrase; 3′-P, 3′-processing; ST, strand transfer; PFV, prototype foamy virus; ASV, avian sarcoma virus; NMR, nuclear magnetic resonance; DKA, diketo acid; FDA, Food and Drug Administration; GIAO, gauge invariant atomic orbitals; DFT, density functional theory; TMS, tetramethylsilane; DMPO, 5,5-dimethylpyrroline-*N*-oxide; LEDGF, lens epithelium-derived growth factor; SSTI, selective strand transfer inhibitor; NNRTI, non-nucleoside reverse transcriptase inhibitor

■ REFERENCES

(1) De Clercq, E. The design of drugs for HIV and HCV. *Nat. Rev. Drug Discovery* **2007**, *6*, 1001–1018.

(2) Andréola, M. L. Closely related antiretroviral agents as inhibitors of two HIV-1 enzymes, ribonuclease H and integrase: "killing two birds with one stone. *Curr. Pharm. Des.* **2004**, *10*, 3713–3723.

(3) Schultz, S. J.; Champoux, J. J. RNase H activity: Structure and function in reverse transcription. *Virus Res.* **2008**, *134*, 86–103.

(4) Chiu, T. K.; Davies, D. R. Structure and function of HIV-1 integrase. *Curr. Top. Med. Chem.* **2004**, *4*, 965–977.

(5) Williams, P. D.; Staas, D. D.; Venkatraman, S.; Loughran, H. M.; Ruzek, R. D.; Booth, T. M.; Lyle, T. A.; Wai, J. S.; Vacca, J. P.; Feuston, B. P.; Ecto, L. T.; Flynn, J. A.; DiStefano, D. J.; Hazuda, D. J.; Bahnck, C. M.; Himmelberger, A. L.; Dornadula, G.; Hrin, R. C.; Stillmock, K. A.; Witmer, M. V.; Miller, M. D.; Grobler, J. A. Potent and selective HIV-1 ribonuclease H inhibitors based on a 1-hydroxy-1,8-naphthyridin-2(1H)-one scaffold. *Bioorg. Med. Chem. Lett.* **2010**, *22*, 6754–6757.

(6) Williams, P. D.; Venkatraman, S.; Langford, H. M.; Kim, B.; Booth, T. M.; Grobler, J. A.; Staas, D.; Ruzek, R. D.; Embrey, M. W.; Wiscount, C. M.; Lyle, T. A. Preparation of 1-hydroxynaphthyridin-2(1H)-one derivatives as anti-HIV agents. PCT Int. Appl. (2008), WO 2008010964 A1 20080124.

(7) Goldgur, Y.; Dyda, F.; Hickman, A. B.; Jenkins, T. M.; Craigie, R.; Davies, D. R. Three new structures of the core domain of HIV-1 integrase: an active site that binds magnesium. *Proc. Natl. Acad. Sci. U.S.A.* **1998**, *95*, 9150–9154.

(8) Golgur, Y.; Craigie, R.; Cohen, G. H.; Fujiwara, T.; Yoshinaga, T.; Fujishita, T.; Sugimoto, H.; Endo, T.; Murai, H.; Davies, D. R. Structure of the HIV-1 integrase catalytic domain complexed with an inhibitor: a platform for antiviral drug design. *Proc. Natl. Acad. Sci. U.S.A.* **1999**, *96*, 13040–13043.

(9) Chen, J. C.; Krucinski, J.; Miercke, L. J.; Finer-Moore, J. S.; Tang, A. H.; Leawitt, A. D.; Stroud, R. M. Crystal structure of the HIV-1 integrase catalytic core and C-terminal domains: a model for viral DNA binding. *Proc. Natl. Acad. Sci. U.S.A.* **2000**, *97*, 8233–8238.

(10) Bujacz, G.; Alexandratos, J.; ZhouLiu, Q.; ClementMella, C.; Wlodawer, A. The catalytic domain of human immunodeificiency virus integrase: ordered active site in the F185H mutant. *FEBS Lett.* **1996**, *398*, 175–178.

(11) Dyda, F.; Hickman, A. B.; Jenkins, T. M.; Engelman, A.; Craigie, R.; Davies, D. R. Crystal structure of the catalytic domain of HIV-1 integrase: similarity to other polynucleotidyl transferases. *Science* **1994**, *266*, 1981–1986.

(12) Greenwald, J.; Le, V.; Butler, S. L.; Bushman, F. D.; Choe, S. The mobility of an HIV-1 integrase active site loop is correlated with catalytic activity. *Biochemistry* **1999**, *38*, 8892–8898.

(13) Maignan, S.; Guilloteau, J. P.; Zhou-Liu, Q.; Clément-Mella, C.; Mikol, V. Crystal structures of the catalytic domain of HIV-1 integrase free and complexed with its metal cofactor: high level of similarity of the active site with other viral integrases. *J. Mol. Biol.* **1998**, *282*, 359–368.

(14) Bujacz, G.; Alexandratos, J.; Wlodawer, A.; Merkel, G.; Andrake, M.; Katz, R. A.; Skalka, A. M. Binding of different divalent cations to the active site of avian sarcoma virus integrase and their effects on enzymatic activity. *J. Biol. Chem.* **1997**, *272*, 18161–18168.

(15) Hare, S.; Gupta, S. S.; Volkov, E.; Engelman, A.; Cherepanov, P. Retroviral intasome assembly and inhibition of DNA strand transfer. *Nature* **2010**, *464*, 232–236.

(16) Davies, J. F., II; Hostomska, Z.; Hostomsky, Z.; Jordan, S. R.; Matthews, D. A. Crystal structure of the ribonuclease H domain of HIV-1 reverse transcriptase. *Science* **1991**, *252*, 88–95.

(17) Arnold, E.; Jacobo-Molina, A.; Nanni, R. G.; Williams, R. L.; Lu, X.; Ding, J.; Clark, A. D., Jr.; Zhang, A.; Ferris, A. L.; Clark, P.; Hizi, A.; Hughes, S. Structure of HIV-1 reverse transcriptase/DNA complex at 7 Å resolution showing active site locations. *Nature* **1992**, *357*, 85–89.

(18) Kohlstaedt, L. A.; Wang, J.; Friedman, J. M.; Rice, P. A.; Steizt, T. A. Crystal structure at 3.5 Å resolution of HIV-1 reverse transcriptase complexed with an inhibitor. *Science* **1992**, *256*, 1783–1790.

(19) Sarafianos, S. G.; Das, K.; Tantillo, C.; Clark, A. D., Jr.; Ding, J.; Whitomb, J. M.; Boyer, P. L.; Hughes, S. H.; Arnold, E. Crystal structure of HIV-1 reverse transcriptase in complex with a polypurine tract RNA: DNA. *EMBO J.* **1992**, *20*, 1449–1461.

(20) Huang, H.; Chopra, R.; Verdine, G. L.; Harrison, S. C. Structure of a covalently trapped catalytic complex of HIV-1 reverse transcriptase: implications for drug resistance. *Science* **1998**, *282*, 1669–1675.

(21) Nowotny, M.; Gaidarnakov, S. A.; Crouch, R. J.; Yang, W. Crystal structures of RNase H bound to an RNA/DNA hybrid: substrate specificity and metal-dependent catalysis. *Cell* **2005**, *121*, 1005–1016.

(22) Nowotny, M.; Gaidarnakov, S. A.; Ghirlando, R.; Cerritelli, S. M.; Crouch, R. J.; Yang, W. Structure of human RNase H1 complexed with an RNA/DNA hybrid: insight into HIV reverse transcription. *Mol. Cell* **2007**, *28*, 264–276.

(23) Pari, K.; Mueller, G. A.; DeRose, E. F.; Kirby, T. W.; London, R. E. Solution structure of the RNase H domain of the HIV-1 reverse transcriptase in the presence of magnesium. *Biochemistry* **2003**, *42*, 639–650.

(24) Grobler, J. A.; Stillmock, K.; Binghua, H.; Witmer, M.; Felock, P.; Espeseth, A. S.; Wolfe, A.; Egbertson, M.; Bourgeois, M.; Melamed, J.; Wai, J. S.; Young, S.; Vacca, J.; Hazuda, D. J. Diketo acid inhibitor mechanism and integrase: implications for metal binding in the active site of phosphotransferase enzymes. *Proc. Natl. Acad. Sci. U.S.A.* **2002**, *99*, 6661–6666.

(25) Hazuda, D. J.; Felock, P.; Witmer, M.; Wolfe, A.; Stillmock, K.; Grobler, J. A.; Espeseth, A.; Gabryelski, L.; Schleif, W.; Blau, C.; Miller, M. D. Inhibitors of strand transfer that prevent integration and inhibit HIV-1 replication in cells. *Science* **2000**, *287*, 646–50.

(26) Tramontano, E.; Esposito, F.; Badas, R.; Di Santo, R.; Costi, R.; La Colla, P. 6-[1-(4-Fluorophenyl)methyl-1*H*-pyrrol-2-yl]-2,4-dioxo-5-hexenoic acid ethyl ester a novel diketo acid derivative which selectively inhibits the HIV-1 viral replication in cell culture and the ribonuclease H activity in vitro. *Antiviral Res.* **2005**, *65*, 117–124.

(27) Zhuang, L.; Wai, J. S.; Embrey, M. W.; Fisher, T. E.; Egbertson, M. S.; Payne, L. S.; Guare, J. P., Jr.; Vacca, J. P.; Hazuda, D. J.; Felock, P. J.; Wolfe, A. L.; Stillmock, K. A.; Witmer, M. V.; Moyer, G.; Schleif, W. A.; Gabryelski, L. J.; Leonard, Y. M.; Lynch, J. J.; Michelson, S. R.; Young, S. D. Design and synthesis of 8-hydroxy-[1,6]-naphthyridines as novel inhibitors of HIV-1 integrase *in vitro* and infected cells. *J. Med. Chem.* **2003**, *46*, 453–456.

(28) Miller, M.; Witmer, M.; Stillmock, K.; Felock, P.; Ecto, L.; Flynn, J.; Schleif, W.; Dornadula, G.; Danovich, R.; Hazuda, D. Biochemical and antiviral activity of MK-0518, a potent HIV integrase inhibitor. In *AIDS 2006—XVI International AIDS Conference; Toronto*. 2006: Oral abstract session: Abstract no. THAA0302.

(29) Klumpp, K.; Hang, J. Q.; Rajendran, S.; Yang, Y.; Derosier, A.; Wong Kai In, P.; Overton, H.; Parkes, K. E. B.; Cammack, N.; Martin, J. A. Two-metal-ion mechanism of RNA cleavage by HIV RNase H and mechanism based design of selective HIV RNase H inhibitors. *Nucleic Acids Res.* **2003**, *31*, 6852–6859.

(30) Didierjean, J.; Isel, C.; Querré, F.; Mouscadet, J. F.; Aubertin, A. M.; Valnot, J. Y.; Piettre, S. R.; Marquet, R. Inhibition of human immunodeficiency virus type 1 reverse transcriptase, RNase H, and integrase activities by hydroxytropolones. *Antimicrob. Agents Chemother.* **2005**, *49*, 4884–94.

(31) Budihas, S. R.; Gorshkova, I.; Daidamakov, S.; Wamiru, A.; Bona, M. K.; Parniak, M. A.; Crouch, R. J.; McMahon, J. B.; Beutler, J. A.; Le Grice, S. F. J. Selective inhibition of HIV-1 reverse transcriptase-associated ribonuclease H activity by hydroxylated tropolones. *Nucleic Acids Res.* **2005**, *33*, 1249–1256.

(32) Marchand, C.; Beutler, J. A.; Wamiru, A.; Budihas, S.; Möllmann, U.; Heinisch, L.; Mellors, J. W.; Le Grice, S. F.; Pommier, Y. Madurahydroxylactone derivatives as dual inhibitors of human immunodeficiency virus type 1 integrase and RNase H. *Antimicrob. Agents Chemother.* **2008**, *52*, 361–4.

(33) Maurin, C.; Bailly, F.; Buisine, E.; Vezin, H.; Mbemba, G.; Mouscadet, J. F.; Cotelle, P. Spectroscopic studies of diketoacids-metal interactions. A probing tool for the pharmacophoric intermetallic distance in the HIV-1 integrase active site. *J. Med. Chem.* **2004**, *47*, 5583–5586.

(34) Sechi, M.; Bacchi, A.; Carcelli, M.; Compari, C.; Duce, E.; Fisicaro, E.; Rogolino, D.; Gates, P.; Derudas, M.; Al-Mawsawi, L. Q.; Neamati, N. From ligand to complexes: inhibition of human immunodeficiency virus type 1 integrase by beta-diketo acid metal complexes. *J. Med. Chem.* **2006**, *49*, 4248–4260.

(35) Bacchi, A.; Biemmi, M.; Carcelli, M.; Carta, F.; Compari, C.; Fisicaro, E.; Rogolino, D.; Sechi, M.; Sippel, M.; Sotriffer, C. A.; Sanchez, T. W.; Neamati, N. From ligand to complexes. Part 2. Remarks on human immunodeficiency virus type 1 integrase inhibition by beta-diketo acid metal complexes. *J. Med. Chem.* **2008**, *51*, 7253–64.

(36) Klumpp, K.; Mirzdegan, T. Recent progress in the design of small molecule inhibitors of HIV RNase H. *Curr. Pharm. Des.* **2006**, *12*, 1909–1922.

(37) Billamboz, M.; Bailly, F.; Barreca, M. L.; De Luca, L.; Mouscadet, J. F.; Calmels, C.; Andreola, M. L.; Christ, F.; Debyser, Z.; Witvrouw, M.; Cotelle, P. Design, synthesis and biological evaluation of a series of 2-hydroxyisoquinoline-1,3(2*H*,4*H*)-diones as dual inhibitors of human immunodeficiency virus type 1 integrase and reverse transcriptase RNase H domain. *J. Med. Chem.* **2008**, *51*, 7717–7730.

(38) Billamboz, M.; Bailly, F.; Lion, C.; Calmels, C.; Andreola, M. L.; Witvrouw, M.; Christ, F.; Debyser, Z.; De Luca, L.; Chimirri, A.; Cotelle, P. 2-Hydroxyisoquinoline-1,3(2*H*,4*H*)-diones as inhibitors of HIV-1 integrase and reverse transcriptase RNase H domain: influence of the alkylation of position 4. *Eur. J. Med. Chem.* **2011**, *46*, 535–546.

(39) Wolinski, K.; Hinton, J. F.; Pulay, P. Efficient implementation of the gauge-independent atomic orbital method for NMR chemical shift calculations. *J. Am. Chem. Soc.* **1990**, *112*, 8251–8260.

(40) Cheeseman, J. R.; Trucks, G. W.; Keith, T. A.; Frish, M. J. A comparison of models for calculating nuclear magnetic resonance shielding tensors. *J. Chem. Phys.* **1996**, *104*, 5497–5509.

(41) Cimino, P.; Gomez-Paloma, L.; Duca, D.; Riccio, R.; Bifulco, G. Comparison of different theory models and basis sets in the calculation of 13C NMR chemical shifts of natural products. *Magn. Reson. Chem.* **2004**, *42*, S26–S33.

(42) Bagno, A.; Rastrelli, F.; Saielli, G. Toward the complete prediction of the ^{1}H and ^{13}C NMR spectra of complex organic molecules by DFT methods: application to natural substances. *Chem.—Eur. J.* **2006**, *12*, 5514–5525.

(43) Frisch, M. J.; Trucks, G. W.; Schlegel, H. B.; Scuseria, G. E.; Robb, M. A.; Cheeseman, J. R.; Montgomery, J. A. Jr.; Vreven, T.; Kudin, K. N.; Burant, J. C.; Millam, J. M.; Lyengar, S. S.; Tomasi, J.; Barone, V.; Mennucci, B.; Cossi, M.; Scalmani, G.; Rega, N.; Petersson, G. A.; Nakatsuji, H.; Hada, M.; Ehara, M.; Toyota, K.; Fukuda, R.; Hasegawa, L.; Ishida, M.; Nakajima, T.; Honda, Y.; Kitao, O.; Nakai, H.; Klene, M.; Li, X.; Knox, J. E.; Hratchian, H. P.; Cross, J. B.; Bakken, V.; Adamo, C.; Jaramillo, J.; Gomperts, R.; Stratmam, R. E.; Yazyev, O.; Austin, A. I.; Cammi, R.; Pomelli, C.; Ochterski, J. W.; Ayala, P. Y.; Morokuma, K.; Voth, G. A.; Salvador, P.; Dannenberg, J. J.; Zakrzewski, V. G.; Dapprich, S.; Daniels, A. D.; Strain, M. C.; Farkas, O.; Malick, D. K.; Rabuck, A. D.; Raghavachari, K.; Foresman, J. B.; Ortiz, L. V.; Cu, Q.; Baboul, A. G.; Clifford, S.; Cioslowski, L.; Stefanov, B. B.; Liu, G.; Liashenko, A.; Piskorz, P.; Komaromi, I.; Martin, R. L.; Fox, D. J.; Keith, T.; Al-Laham, M. A.; Peng, C. Y.; Nanayakkara, A.; Challacombe, M.; Gili, P. M. W.; Johnson, B.; Chen, W.; Wong, M. W.; Gonzalez, C.; Popie, J. A. Gaussian 03, Revision C.02; Gaussian, Inc.: Wallingford, CT, 2004.

(44) Schuler, R. H.; Albarran, G.; Zajicek, J.; George, M. V.; Fessenden, R. W.; Carmichael, I. On the addition of $^{\bullet}$OH radicals to the ipso positions of alkyl-substituted aromatics: production of 4-hydroxy-4-methyl-2,5-cyclohexadien-1-one in the radiolytic oxidation of *p*-cresol. *J. Phys. Chem. A* **2002**, *106*, 12178–12183.

(45) Wipf, P.; Kerekes, A. Structure reassignment of the fungal metabolite TAEMC161 as the phytotoxin viridiol. *J. Nat. Prod.* **2003**, *66*, 716–718.

(46) Timmons, C.; Wipf, P. Density functional theory calculation of ^{13}C NMR shifts of diazaphenanthrene alkaloids: reinvestigation of the structure of samoquasine A. *J. Org. Chem.* **2008**, *73*, 9168–9170.

(47) Sarotti, M.; Pellegrinet, S. A Multi-standard approach for GIAO ^{13}C NMR calculations. *J. Org. Chem.* **2009**, *74*, 7254–7260.

(48) Christ, F.; Voet, A.; Marchand, A.; Nicolet, S.; Desimmie, B. A.; Marchand., D.; Bardiot, D.; Van der Veken, N. J.; Van Remoortel, B.; Strelkov, S. V.; De Maeyer, M.; Chaltin, P.; Debyser, Z. Rational design of first-in-class inhibitors in the LEDGF/p75-integrase interaction and HIV replication. *Nat. Chem. Biol.* **2010**, *6*, 442–448.

(49) Delelis, O.; Malet, I.; Na, L.; Tchertanov, L.; Calvez, V.; Marcelin, A. G.; Subra, F.; Deprez, E.; Mouscadet, J. F. The G140S mutation in HIV integrases from raltegravir-resistant patients rescues catalytic defect due to the resistance Q148H mutation. *Nucleic Acids Res.* **2009**, *37*, 1193–1201.

(50) Nunberg, J. H.; Schleif, W. A.; Boots, E. J.; O'Brien, J. A.; Quintero, J. C.; Hoffman, J. M.; Emini, E. A.; Goldman, M. E. Viral resistance to human immunodeficiency virus type 1-specific pyridinone reverse transcriptase inhibitors. *J. Virol.* **1991**, *65*, 4887–4892.

(51) Ames, D. E.; Grey, T. F. 3-Hydroxyimides. II. Derivatives of homophthalic and phthalic acids. *J. Chem. Soc.* **1955**, 3518–3521.

(52) Strashnova, S. B.; Kovalchukova, O. V.; Zaitsev, B. E.; Stash, A. Complexation of 2,3-dihydroxyquinoline with some bivalent d metals. Crystal and molecular structures of 2,3-dihydroxyquinoline. *Russ. J. Coord. Chem.* **2008**, *34*, 775–779.

(53) Vezin, H.; Lamour, E.; Routier, S.; Villain, F.; Bailly, C.; Bernier, J. L.; Catteau, J. P. Free radical production by hydroxy-salen manganese complexes studied by ESR and XANES. *J. Inorg. Biochem.* **2002**, *92*, 177–182.

(54) Tewtrakul, S.; Miyashiro, H.; Nakamura, N.; Hattori, M.; Kawahata, T.; Otake, T.; Yoshinaga, T.; Fujiwara, T.; Supavita, T.; Yuenyongsawad, S.; Rattanasuwon, P.; Dej-Adisai, S. HIV-1 integrase inhibitory substances from *Coleus parvifolius*. *Phytother. Res.* **2003**, *17*, 232–239.

(55) Billamboz, M.; Bailly, F.; Cotelle, P. Facile synthesis of 4-alkoxycarbonylisoquinoline-1,3-diones and 5-alkoxycarbonyl-2-benzazepine-1,3-diones via a mild alkaline cyclization. *J. Heterocycl. Chem.* **2009**, *46*, 392–398.

(56) Debyser, Z.; Cherepanov, P.; Pluymers, W.; De Clercq, E. Assays for the evaluation of HIV-1 integrase inhibitors. *Methods Mol. Biol.* **2001**, *160*, 139–155.

(57) Hwang, Y.; Rhodes, D.; Bushman, F. Rapid microtiter assays for poxvirus topoisomerase, mammalian type IB topoisomerase and HIV-1 integrase: application to inhibitor isolation. *Nucleic Acids Res.* **2000**, *28*, 4884–4892.

(58) Busschots, K.; Voet, A.; De Mayer, M.; Rain, J. C.; Emiliani, S.; Benarous, R.; Desender, L.; Debyser, Z.; Christ, F. Identification of the LEDGF/p75 binding site in HIV-1 integrase. *J. Mol. Biol.* **2007**, *365*, 1480–1492.

(59) Moelling, K.; Schulze, T.; Diringer, H. Inhibition of human immunodeficiency virus type 1 RNase H by polysulfated polyanions. *J. Virol.* **1989**, *63*, 5489–5491.

(60) Dufour, E.; Reinbolt, J.; Castroviejo, M.; Ehresmann, B.; Litvak, S.; Tarrago-Litvak, L.; Andreola, M. L. Cross-linking localization of a HIV-1 reverse transcriptase peptide involved in the binding of primer tRNALys3. *J. Mol. Biol.* **1999**, *285*, 1339–1346.

(61) Pauwels, R.; Balzarini, J.; Baba, M.; Snoeck, R.; Schols, D.; Herdewijn, P.; Desmyter, J.; De Clercq, E. Rapid and automated tetrazolium-based colorimetric assay for the detection of anti-HIV compounds. *J. Virol. Methods* **1988**, *20*, 309–321.